Journal of Zhejiang University-SCIENCE A (Applied Physics & Engineering)
ISSN 1673-565X (Print); ISSN 1862-1775 (Online)
www.zju.edu.cn/jzus; www.springerlink.com
E-mail: jzus@zju.edu.cn

Model tests on interaction between soil and geosynthetics subjected to localized subsidence in landfills*

Bin ZHU†, Deng GAO, Jun-chao LI, Yun-min CHEN

(*MOE Key Laboratory of Soft Soils and Geoenvironmental Engineering, Department of Civil Engineering, Zhejiang University, Hangzhou 310058, China*)

†E-mail: zhubin_ccea@yahoo.com.cn

Received Nov. 15, 2011; Revision accepted Mar. 26, 2012; Crosschecked May 15, 2012

Abstract: In a landfill, excessive tensile strains or failure of the liner system due to localized subsidence underneath the geosynthetic liner, is a concern in design and operation of the landfill. The localized subsidence can be commonly withstood by reinforcements such as geogrids. A total of nine model tests were carried out to study the influence of soil arching in overburden sandy soil on the geosynthetics and the interaction between the soil and the geosynthetics. The localized subsidence was modeled by a strip trapdoor under the geosynthetic reinforcements. The reinforcement includes several layers of polyvinylchlorid (PVC) membrane or both PVC membrane and a compacted clay layer. Test results show that the vertical soil pressure acting on the geosynthetics within the subsidence zone is strongly related to the deflection of the geosynthetics. The soil pressure acting on the deflected geosynthetics will decrease to a minimum value with respect to its deflection if the final deflection is large enough, and this minimum value is almost independent of the overburden height. Otherwise, the deflection of geosynthetics cannot result in a full degree of soil arching, and the soil pressure within the subsidence zone increases with the increase of overburden height. Deflections and strains of the geosynthetics obviously decrease with the increase of their tensile stiffness. The presence of a compacted clay layer buffer can therefore reduce both deflections and strains of the geosynthetics. Finally, a composite liner structure is recommended for landfills to withstand the localized subsidences.

Key words: Landfill, Soil arching, Trapdoor, Model test, Geosynthetics
doi:10.1631/jzus.A1100315 **Document code:** A **CLC number:** TU411.93

1 Introduction

The security of engineering projects is often a concern during the siting, construction and maintenance of facilities in areas that contain sinkholes. However, some sinkholes cannot be detected, or appear after the construction of buildings or structures. The sinkholes mentioned above originate either from natural phenomena mainly like rock dissolution by water with a high carbon dioxide content (Karstic cavities), or from human activities related to the extraction of minerals.

The composite liner system lying on the bottom of the landfill is used to prevent leakage of the leachate (Hu and Chen, 2001). Localized subsidence arising from a sinkhole underlying the liner system could potentially lead to excessive tensile strains in the geosynthetic sealing materials in the liner system and even result in geosynthetic rupture. An intermediate liner system between the old and new landfill is recommended for vertically expanded landfills in China. For this intermediate liner system, conditions causing its localized subsidence include degradation of large goods and collapse of waste with large voids, such as barrels, household appliances, and furniture. Therefore, it is important to design an effective liner system withstanding such localized subsidences (Qian *et al*., 2001).

* Project supported by the National Basic Research Program of China (No. 2012CB719800), the National Natural Science Foundation of China (No. 51127005), and the Key Innovative Team Program of Zhejiang Province (No. 2009R50050), China

Geogrid reinforcements are often used in landfills to withstand the underneath localized subsidence. Several design methods have been successively developed (Giroud *et al.*, 1990; Kuo *et al*., 2005). One of the most important issues is how to calculate the soil pressure acting on the liner system taking into account the soil arching effect. After Terzaghi (1943) presented a trapdoor experiment to investigate the soil arching effect, a series of laboratory-scale and in-situ tests has been carried out to study the reinforcing effects in pile-supported embankments (Chew *et al*., 2006; van Eekelen *et al*., 2007; Chen *et al*., 2008; Chen R.P. *et al*., 2010). There are two main differences of geosynthetic reinforcements between pile-supported embankments and landfills: (1) the overburden height of the geosynthetics in the landfill is much larger than that of the pile-supported embankment. (2) the tensile strains of geosynthetic reinforcements should be within the limits of the allowable tensile strains of the protected sealing materials in the liner system.

Besides the reinforcement method mentioned above, a layer of compacted soil or selected waste underlying the liner system can be used as a "buffer" to withstand the underneath localized subsidence (Jessberger and Stone, 1991; Jang and Montero, 1993). The compacted clay layer can also serve as a sealing material against leakage of the leachate. It is required to study the mechanism of reducing strains and deflections of the geosynthetics by the compacted clay buffer, in order to give optimal liner structures for engineering practices.

In this paper, several model tests with a strip trapdoor are carried out to study both the soil arching effect and the soil-geosynthetic interaction subjected to underneath localized subsidence in landfills, as shown in Fig. 1. In Fig. 1, p is the vertical soil pressure; b is the width of localized subsidence; H is the height of over-laying soil; and γ is the unit weight of over-laying soil. The effects of the filling height, the tensile stiffness of geosynthetics and the compacted clay layer are investigated in detail.

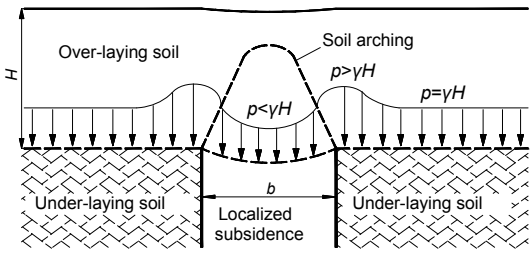

Fig. 1 Illustration of localized subsidence

2 Model test set-up

2.1 Test set-up

As shown in Fig. 2a, the test set-up consists of a rigid base, a subsidence simulator and a tank. The tank is 1.2 m in length, 1 m in width, and 2 m in height. Toughened glasses were used in the front and back walls of the tank for easy observation. Steel plates were used in the right and left walls and the surfaces were lubricated with epikote to limit frictional effects. The subsidence simulator consists of a reductor, a drive chain, two pillows, and a steel trapdoor with 0.2 m in width (Fig. 2b). The contact surface between the trapdoor and the rigid base was lubricated with vaseline. Through turning the handle of the reductor by hand, the trapdoor can move up and down synchronously with a speed of 0.17 mm per cycle, nearly 0.034 mm/s.

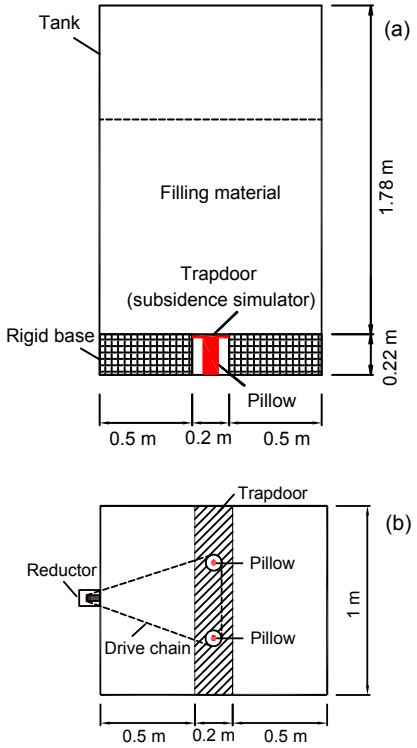

Fig. 2 Lay out of test set-up
(a) Front view; (b) Top view

2.2 Test program

It was found that the shear strength of the deep municipal solid waste in a landfill is similar to that of sand (Zhan *et al*., 2008). As shown in Fig. 3, the overburden filling material on the geosynthetics is sandy soil, and the reinforcement layer on the localized subsidence includes several layers of PVC membrane or both PVC membrane and a compacted clay layer. Here, E_t is the tensile stiffness of geosynthetic reinforcements, and y is the deflection of the geosynthetic. The test program is listed in Table 1 in detail. Tests 1–6 were carried out for studying the effects of filling height and tensile stiffness of geosynthetics on soil arching and soil-geosynthetic interaction (Fig. 3a). The model tests using sandy soil were carried out for four different overburden heights, i.e., H=0.4 m, 0.8 m, 1.2 m, and 1.6 m, respectively. Three different tensile stiffness of geosynthetics values were used in the model tests (4.7, 9.4, and 14.1 kN/m), taking one, two, and three layers of membranes in tests, respectively. Tests 7–9 were carried out to investigate the mechanism of strains and deflections of the geosynthetics by a compacted clay buffer (Fig. 3b). The thickness values of the compacted clay layer and sandy soil are 0.04 m and 1.6 m, respectively.

2.3 Test materials and equipments

The sandy soil used in Tests 1–9 was taken from Qiantang River Beach, Hangzhou, China. Its specific gravity G=2.65, the coefficient of uniformity C_u=1.82, and other parameters are D_{10}=0.088 mm, D_{60}=0.16 mm, e_{max}=1.01, and e_{min}=0.52. The test bed was prepared by pluviation at a dry unit weight of 14.09–14.31 kN/m^3, corresponding to a relative density of (60±5)%. The friction angle of the sand at the relative density of 60% as measured through direct shear tests is 34.16°.

In Tests 7–9, a natural clay soil in Hangzhou was used to prepare the compacted clay layer. The liquid limit, plastic limit, plasticity index and specific gravity of the clay soil is found to be 37.9%, 20.9%, 17%, and 2.73, respectively. It was pulverized and mixed with pre-determined amount of water, and then was placed in the test box using a metal scoop and compacted in two sub-layers with 0.02 m thickness in each case. Each sub-layer was compacted by a wood hammer with a compacting energy of 324 kJ/m^3. The moisture content of the compacted clay is in the range of 23.1%–24.5% and its bulk unit weight is in the range of 15.8–16.2 kN/m^3. It has a cohesion c_{cu} of 13.8 kPa and an internal friction angle φ_{cu} of 19.5°.

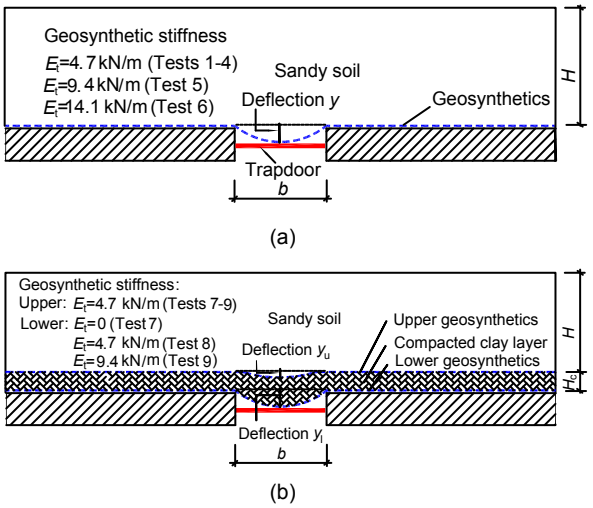

Fig. 3 Illustration of Tests 1–6 (a) and Tests 7–9 (b)

Table 1 Test program

Filling material	Test number	H (m)	b (mm)	E_t (kN/m)	H_c (m)
Sandy soil	1	0.4	0.2	4.7	–
	2	0.8	0.2	4.7	–
	3	1.2	0.2	4.7	–
	4	1.6	0.2	4.7	–
	5	1.6	0.2	9.4	–
	6	1.6	0.2	14.1	–
Sandy soil+ compacted clay layer	7	1.6	0.2	4.7	0.04
	8	1.6	0.2	9.4	0.04
	9	1.6	0.2	14.1	0.04

A 0.18 mm-thick PVC membrane was used as the reinforcing geosynthetics in Tests 1–9. Its tensile strength as obtained by the wide-width strip method (ASTM Standard D4595-2009) is 0.47 kN/m at the axial strain of 10%. One layer of PVC membrane was placed in Tests 1–4 and Test 7, and two layers in Test 5 and Test 8, three layers in Test 6 and Test 9. The creep effects of the geosynthetic material were not considered in this study. To investigate the variation of soil pressures acting on the geosynthetics, nine miniature pressure transducers (PTs) (CYG712) with a measuring range of 100 kPa and a sensitivity of 0.25%FS were placed on the geosynthetics as shown in Fig. 4. A data acquisition system (Fluke 2680) was used to automatically collect the data. In this study,

test data of PT1, PT2, PT3, and PT4 are the average values of PT1a–1c, PT2a and PT2b, PT3a and PT3b, PT4a and PT4b, respectively.

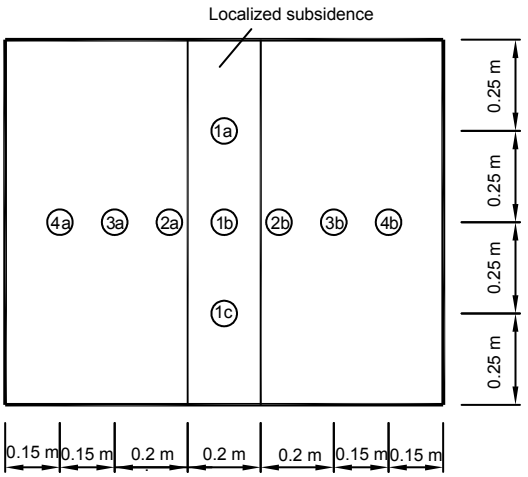

Fig. 4 Arrangement of pressure transducers (PTs)

2.4 Test procedure

Different layers of membranes modeling the geosynthetics with different tensile stiffness were placed on the rigid base and anchored at each edge of the localized subsidence with glue, which means that the membrane elongation beyond the localized subsidence zone was not considered as the same way of Giroud *et al*. (1990). The length of the geosynthetics that is pulled out from the horizontal zone beyond the localized subsidence zone is strongly related to the burden pressure (Zhu *et al*., 2009). It was found that its value for the vertical expanded landfill is smaller than that of the cover system mainly due to the fact that their burden pressures on the geosynthetics are much different. This study mainly deals with the problem of vertical expanded landfill. Eleven markers were placed in the pre-determined locations on the membranes (Fig. 5) so that the membrane strains can be calculated. Then, nine PTs were placed on the membranes. After the overburden filling height was reached, the subsidence simulator was dropped down in several stages and the stable readings of PTs were recorded in every stage.

2.5 Discussion of scaling effect

The strain of geosynthetics, ε can be expressed as

$$\varepsilon = f(p, b, E_t) = f(\gamma, H, b, E_s, \nu, \varphi, E_t), \quad (1)$$

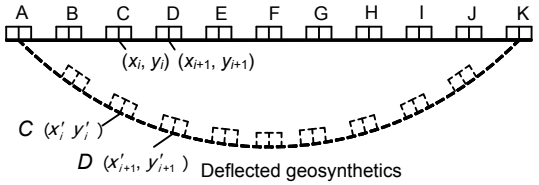

Fig. 5 Initial and final positions of deflected geosynthetics

where E_s is the modulus of filling material; ν is the Poisson's ratio of filling material; and φ is the internal frictional angle of filling material. Eq. (1) can be rewritten as the following dimensionless form:

$$\varepsilon = f\left(\frac{H}{b}, \frac{E_s}{\gamma b}, \nu, \varphi, \frac{E_t}{\gamma b^2}\right). \quad (2)$$

Based on Eq. (2), the scaling criterion between the prototype and the model can be given as

$$\left(\frac{H}{b}\right)_p = \left(\frac{H}{b}\right)_m, \quad (3)$$

$$\left(\frac{E_s}{\gamma b}\right)_p = \left(\frac{E_s}{\gamma b}\right)_m, \quad (4)$$

$$\left(\frac{p}{\gamma b}\right)_p = \left(\frac{p}{\gamma b}\right)_m, \quad (5)$$

$$\left(\frac{y}{b}\right)_p = \left(\frac{y}{b}\right)_m, \quad (6)$$

$$\left(\frac{E_t}{\gamma b^2}\right)_p = \left(\frac{E_t}{\gamma b^2}\right)_m, \quad (7)$$

$$\nu_p = \nu_m, \quad (8)$$

$$\varphi_p = \varphi_m, \quad (9)$$

$$\varepsilon_p = \varepsilon_m. \quad (10)$$

The scaling factors could be deduced by Eqs. (3)–(10) as shown in Table 2, where n is the scale between the prototype and the model. These scaling relationships in Table 2 are recommended to be served as scaling factors of proposed model tests, but neglecting the scaling effect of the modulus of filling material and influence of soil gravity on the soil arching effect. Rigorous scaling factors of the proposed tests at 1g proved difficult to ascertain.

Table 2 Scaling factors of proposed model tests

Parameter	Suggested scaling factor
Width of localized subsidence, b	$1/n$
Filling height, H	$1/n$
Poisson's ratio, v	1
Vertical soil pressure in subsidence zone, p/γ	$1/n$
Deflection of geosynthetics, y	$1/n$
Strain of geosynthetics, ε	1
Tensile stiffness of geosynthetics, E_t/γ	$1/n^2$

3 Tests without a compacted clay layer

3.1 Soil pressures on geosynthetics

Fig. 6 shows the variation of soil pressures acting on the geosynthetics for Test 1 and Test 4. The measured values of PT1–PT4 were given in the two plots. It can be seen that the soil pressure acting on the deflected geosynthetics (PT1 readings) decreases gradually and tends to a stable value. For a low filling height (i.e., H=0.4 m), the soil pressure of PT2 increases significantly, while PT3 and PT4 readings keep almost constant. However, if the filling height is relatively large (i.e., H=1.6 m), PT3 and PT4 readings increase by 21.94% and 27.62%, respectively. Thus, it may be concluded that the development of the soil arching effect is related to filling height of the soil. The larger the filling height is, the more soil pressures will be transferred from the subsidence zone to the nearby zone.

Fig. 7a shows the variation of the PT1 readings for different filling heights. It is obvious that the soil pressure acting on the geosynthetics is strongly related to its deflection. The soil arching was fully formed when the PT1 readings keep almost stable (i.e., the maximum deflection of the geosynthetics y≥15 mm). In this state, very limited pressures will be further transferred from the subsidence zone to the nearby zone. The final soil pressures are 0.96 kPa (H=0.4 m), 1.15 kPa (H=0.8 m), 1.20 kPa (H=1.2 m), and 1.04 kPa (H=1.6 m), respectively. These values are similar to each other. Thus, the final soil pressure

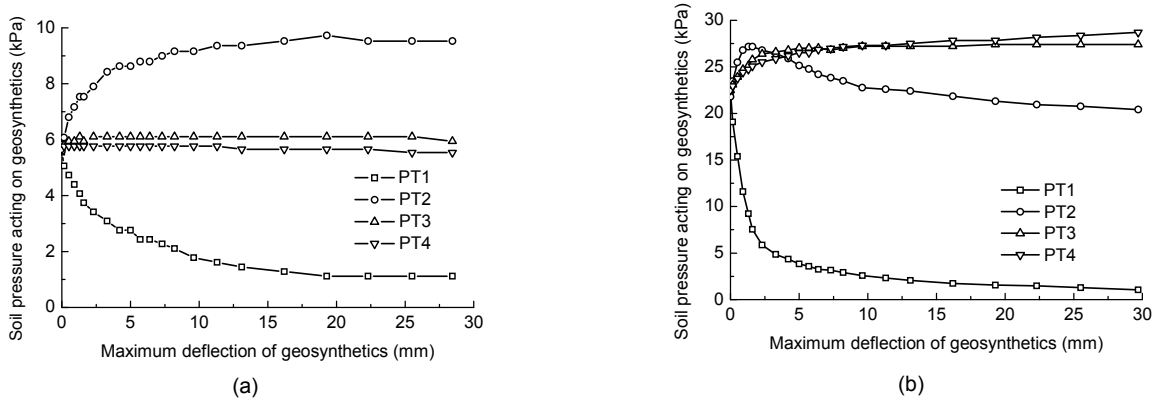

Fig. 6 Variation of soil pressures acting on geosynthetics for different filling heights
(a) Test 1 (H=0.4 m, E_t=4.7 kN/m); (b) Test 4 (H=1.6 m, E_t=4.7 kN/m)

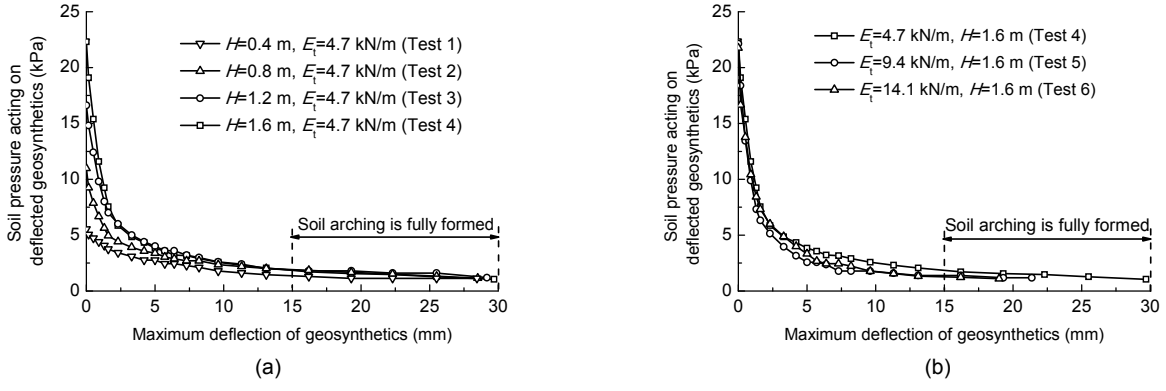

Fig. 7 Effects of filling height (a) and tensile stiffness of geosynthetics (b) on soil pressures of PT1

acting on the deflected geosynthetics is almost independent of the filling height, on condition that the deflection of geosynthetics is sufficient to result in full degree of soil arching.

Fig. 7b shows the variation of the PT1 readings for different values of geosynthetic stiffness. The three curves are quite similar and the final soil pressures are 1.04 kPa (E_t=4.7 kN/m), 1.19 kPa (E_t= 9.4 kN/m), and 1.09 kPa (E_t=14.1 kN/m), respectively. The average value of the final soil pressures is 1.10 kPa. It is concluded that the final soil pressure acting on the deflected geosynthetics is almost independent of their total tensile stiffness in these tests. It can be seen that the soil arching was fully formed in the three tests, since the final maximum deflection of the geosynthetics are large enough. For an extreme case in which the geosynthetic stiffness is infinite large, there will be no deflection for the geosynthetics. As a result, there will be no soil arching effect and the soil pressure acting on the geosynthetics will be equal to the self-weight vertical stress of the overburden soil.

3.2 Vertical and horizontal soil pressures inside overburden soil

As shown in Fig. 8, four additional PTs were placed at point *A* and point *B* in Test 5. The vertical dice between point *A* and the trapdoor is 0.2 m, and the distance for point *B* is 1.2 m. With the development of deflections of the geosynthetics, the vertical soil pressure at point *A* decreases gradually and finally tends to keep constant. The horizontal soil pressure at point *A* increases at the beginning and then exceeds the soil vertical pressure, which means that the rotation of principal stress axes of the soil has occurred. However, the horizontal soil pressure is always smaller than the vertical soil pressure at point *B*, even when it increases continuously with the development of the deflection of the geosynthetics. Thus, the larger the distance between the deflected geosynthetics and the position inside soil is, the less the variation of the soil pressure will occur. For point *B* in Test 5, even its vertical soil pressure has no significant change, the stress redistribution also occurred since its horizontal soil pressure increases obviously subjected to the localized subsidence.

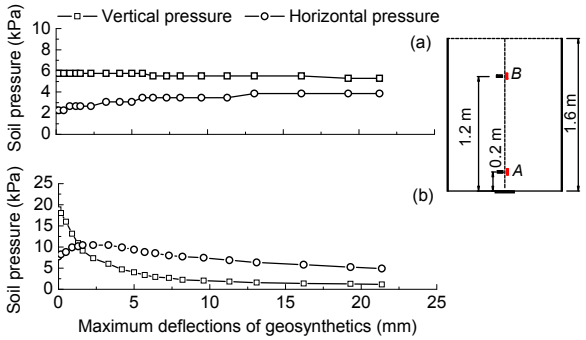

Fig. 8 Vertical and horizontal soil pressures inside soil at point *B* (a) and point *A* (b) in Test 5 (*H*=1.6 m, E_t=9.4 kN/m)

3.3 Deflections and strains of geosynthetics

Fig. 9a shows the effect of filling height on final deflected shape of the geosynthetics. The final deflections of the geosynthetics for *H*=0.4 m, 0.8 m, 1.2 m, and 1.6 m are 28.45 mm, 28.50 mm, 29.17 mm, and 29.69 mm, respectively. According to the tensioned membrane theory (Giroud *et al.*, 1990), equal final soil pressures acting on the deflected geosynthetics will result in the same final deflections of geosynthetics when the tensile stiffness of the geosynthetics is constant. Fig. 9b shows the effect of tensile stiffness of the geosynthetics on its final deflected shape. The final maximum deflections of the geosynthetics are 21.38 mm and 19.00 mm for the two tensile stiffness E_t=9.4 kN/m and 14.1 kN/m, respectively. Thus, it may be concluded that the deformation of the sandy soil will be reduced by increasing the tensile stiffness of the geosynthetics.

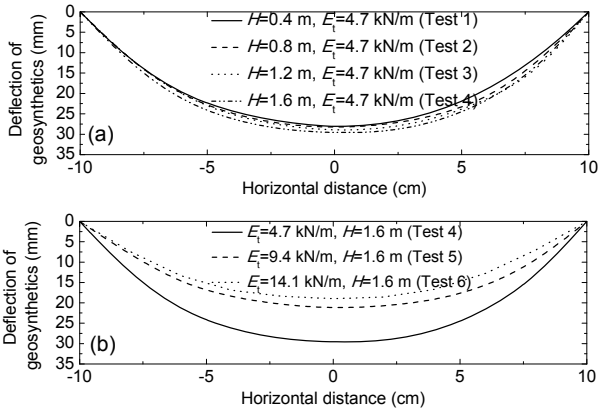

Fig. 9 Effects of filling height (a) and tensile stiffness of geosynthetics (b) on final deflected shape of geosynthetics

Strain distribution of the geosynthetics was recorded through 11 different markers placed on the geosynthetics (Fig. 5), using the digital image analysis (DIA) method (Zornberg and Arriaga, 2003; Viswanadham and Mahajan, 2007). The strains between two markers can be calculated by comparing their initial distance and final distance. For any two adjacent markers with initial coordinates $C(x_i, y_i)$ and $D(x_{i+1}, y_{i+1})$, they will be displaced to new positions after subsidence, with final coordinates $C(x_i', y_i')$ and $D(x_{i+1}', y_{i+1}')$. Thus, the strain in segment CD can be obtained as

$$\varepsilon_{CD} = \sqrt{\frac{(x_{i+1}' - x_i')^2 + (y_{i+1}' - y_i')^2}{(x_{i+1} - x_i)^2 + (y_{i+1} - y_i)^2}} - 1. \quad (11)$$

Here take segment CD in Test 1 as an example (Fig. 10). The coordinates of points C and D are: before deformation, C (3.884 cm, 0.00), D (5.904 cm, 0.00); after deformation, C' (3.697 cm, 2.322 cm), D' (5.784 cm, 2.695 cm). Thus, the tension strain of segment CD is ε_{CD}=4.95%.

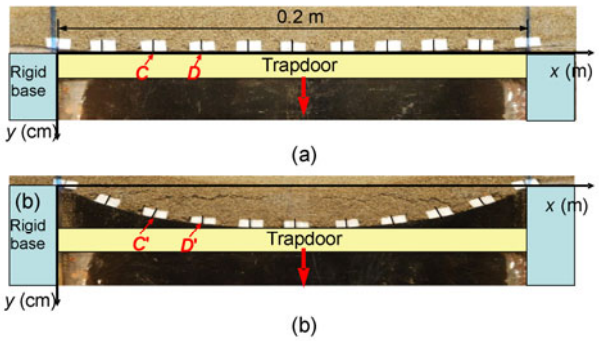

Fig. 10 Initial (a) and final (b) positions of geosynthetics in Test 1

The average strain of the deflected geosynthetics can be expressed by the arch elongation method as

$$\varepsilon_{ave} = \frac{L'}{L} - 1, \quad (12)$$

where L is the initial length, and L' is the final arc length of the section AK.

The geosynthetic strains are evaluated as shown in Fig. 11. The strains at edges of the deflected geosynthetics are generally larger than those in the middle part, while the tensioned membrane theory of Giroud *et al*. (1990) assumes that the strains are uniform throughout the deflected geosynthetics (Villard and Briançon, 2008; Briancon and Villard, 2008). This can be explained as follows. With sinking of the trapdoor, the edges of the geosynthetics in the subsidence zone will be separated from the trapdoor and begin to deform earlier, while the middle part of the geosynthetics will keep contact with the trapdoor at the moment and does not deform until the trapdoor is fully sunk. The average strains of the geosynthetics in Tests 1–6 are 5.30%, 5.41%, 5.76%, 5.96%, 3.20%, and 2.38%, respectively. It can be seen that the average strain of the geosynthetics dramatically decreases with the increase in its tensile stiffness.

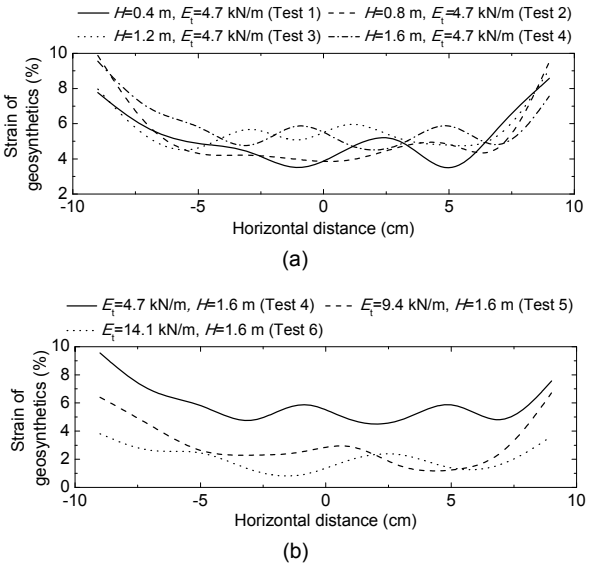

Fig. 11 Effects of filling height (a) and tensile stiffness of geosynthetics (b) on strains of geosynthetics

3.4 Comparisons between calculated and test results

A reinforcement design method has been developed considering the soil arching theory, based on the tensioned membrane theory (Giroud *et al*., 1990). The calculation formulae are expressed as

$$p = \frac{\gamma b}{2K \tan \varphi}(1 - e^{-2K \tan \varphi (H/b)}), \quad (13)$$

$$T = E_t \varepsilon = pr\Omega, \quad (14)$$

where T is the tensile load of geosynthetics; K is the coefficient of lateral earth pressure; Ω is the dimensionless factor related to the maximum deflection y or strain ε of the geosynthetics. With the assumptions that the strain in the portion of the geosynthetics overlying the void is uniformly distributed and the geosynthetics does not slide toward the void, the following expressions are given by (Giroud *et al*., 1990)

$$\Omega = (1/4)[2y/b + b/(2y)], \quad (15)$$

$$1+\varepsilon = 2\Omega \arcsin[1/(2\Omega)], \ y/b \le 0.5. \quad (16)$$

Eq. (13) is the classical expression of the soil pressure proposed by Terzaghi (1943). Since the stress state of the soil in the arching zone has not been fully understood, different values of lateral earth pressure coefficient (K) are proposed, as shown in Table 3. Terzaghi (1943) referred to K as "an empirical coefficient" and took it equal to 1, Aubertin *et al.* (2003) considered K as the passive pressure coefficient, Chen R.X. *et al*. (2010) proposed a modified lateral earth pressure coefficient considering rotations of principal stress axes of soil in the arching effect zone, and Giroud *et al*. (1990) preferred Handy (1985)'s K.

Table 3 Available expressions of K

Reference	Expression of K
Terzaghi (1943)	K=1
Giroud *et al*. (1990)	$K=1.06(\cos^2\theta+K_a\sin^2\theta)$, $\theta=45°+\varphi/2$
Aubertin *et al*. (2003)	$K=K_p=\tan^2(45+\varphi/2)$
Chen R.X. *et al*. (2010)	$K=(\cos^2\theta+K_p\sin^2\theta)/(\sin^2\theta+K_p\cos^2\theta)$, $\theta=45°+\varphi/2$

Fig. 12 shows a comparison of soil pressures acting on the geosynthetics calculated by different methods. If the deflection of the geosynthetics is sufficient to result in full degree of soil arching (i.e., y=28 mm, which is equal to that of the trapdoor), the calculated soil pressures using the K proposed by Terzaghi (1943), Aubertin *et al*. (2003), and Chen R.X. *et al*. (2010) are acceptable compared with the test results. On the other hand, the method of Giroud *et al*. (1990) gives over-conservative soil pressures. However, if the deflection of the geosynthetics is not sufficient to result in full degree of soil arching (i.e., y=0.9 mm, which is the same to that of the trapdoor), all available methods underestimate the soil pressures, especially for the case with a large filling height (i.e., H=1.6 m).

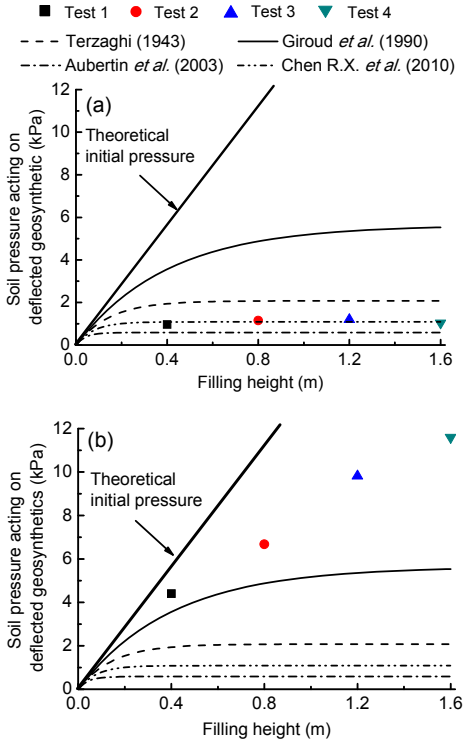

Fig. 12 Comparisons of soil pressures for y=28 mm (a) and 0.9 mm (b)

For the vertical landfill expansion, the vertically expanded waste fill is generally dozens of meters in height and the theoretical initial pressure acting on the composite liner is quite large. If the allowable deflection of the composite liner is not sufficient to develop a full degree of soil arching in the waste fill, the actual soil pressures acting on the composite liner may be far more than those calculated by the available methods, indicating that these methods may underestimate results in this situation.

Combining Eq. (14) with Eq. (15), the following relation can be obtained:

$$E_t\{2\Omega \arcsin[1/(2\Omega)] - 1\} = pb\Omega. \quad (17)$$

With the known E_t and b, the dimensionless factor Ω can be calculated by Eq. (17). Then the maximum deflection y and strain ε of the geosynthetics can be obtained by Eqs. (15) and (16), respectively. Fig. 13

shows the comparison of final maximum deflection and average strain between calculated and test results. It can be seen that the calculated results by the tensioned membrane theory of Giroud *et al*. (1990) are consistent with the test results. With the increase of tensile stiffness of the geosynthetics, the deflection and average strain decrease rapidly, provided that the tensile stiffness is small. However, if the tensile stiffness of the geosynthetics is relatively large (i.e., $E_t \geq 10$ kN/m), the reinforcement effect of geosynthetics is not so significant. Thus, for a considered localized subsidence with a width of 1.8 m, it is recommended to choose geosynthetic reinforcements without a relatively large tensile stiffness to save the investment. Fig. 14 shows the comparison of final deflected shape of the geosynthetics in Test 6. The calculated and test results are in good agreement with each other. Note that the method of Giroud *et al*. (1990) assumed that the deflected shape of geosynthetics is with an arc-cross section.

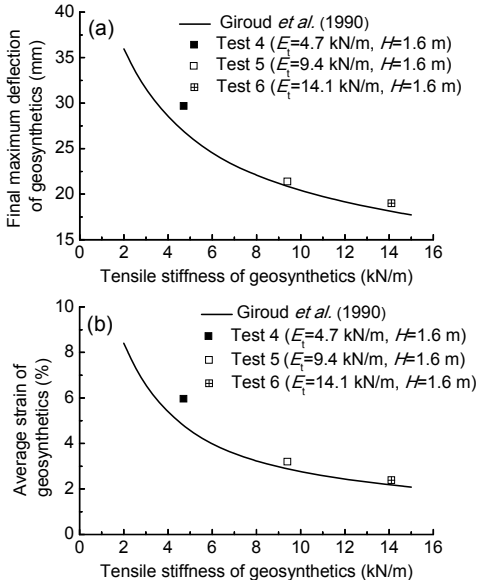

Fig. 13 Comparisons of final maximum deflection (a) and strain of geosynthetics (b)

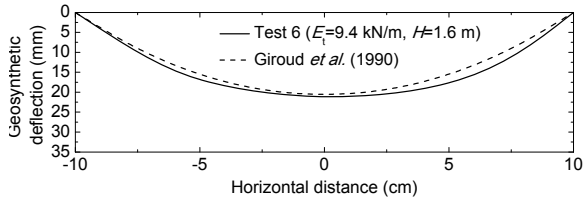

Fig. 14 Comparisons of final deflected shape of geosynthetics

4 Tests with a compacted clay layer

4.1 Soil pressures acting on the upper geosynthetics

Fig. 15 shows the variation of soil pressures acting on the upper geosynthetics in Test 8 and Test 9. Due to the existence of the compacted clay layer, the deflection of the upper geosynthetics is less than that of the lower geosynthetics (or the trapdoor displacement). It can be seen that the variation of PT1–PT4 readings in the two figures is generally similar with that depicted in Fig. 6.

Fig. 16 shows the variation of soil pressures of PT1 with respect to the trapdoor displacement. The final soil pressure acting on the deflected upper geosynthetic in Test 7 is 1.10 kPa, which is close to the measured values in Tests 1–6. This is because the deflection of the upper geosynthetic is sufficient to result in full degree of soil arching in Test 7, and the final soil pressure can reach a minimum value. However, the final soil pressures acting on the deflected upper geosynthetics in Test 8 and Test 9 are 2.5 kPa and 2.63 kPa, respectively, which means that the deflections of the upper geosynthetics are not sufficient enough to result in full degree of soil arching.

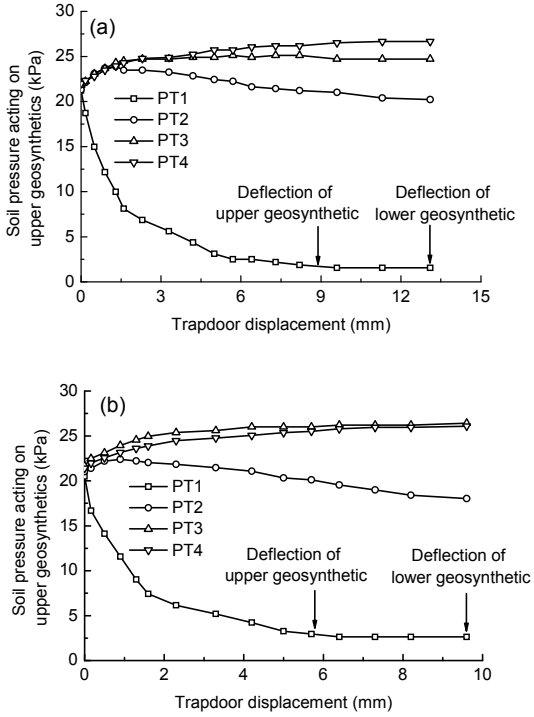

Fig. 15 Variations of soil pressures acting on upper geosynthetics in Test 8 (a) and Test 9 (b)

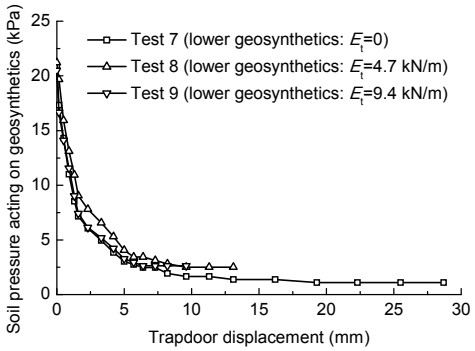

Fig. 16 Soil pressures of PT1 in Tests 7–9

4.2 Deflections and strains of geosynthetics

Figs. 17a–17c show deformations of the geosynthetics and the compacted clay layers. In Fig. 17a, the compacted clay layer in Test 7 without any lower geosynthetics collapsed during its deflection. As a result, the compacted clay layer will lose its function as a buffer or a sealing material or both. Subsequently cracks appeared in the middle and the edges of the compacted clay layer, over the trapdoor. As shown in Figs. 17b and 17c, if the lower geosynthetic reinforcement was placed, the cracks in the compacted clay layer decreased significantly, especially for the test with relatively large geosynthetic reinforcement (i.e., Test 9).

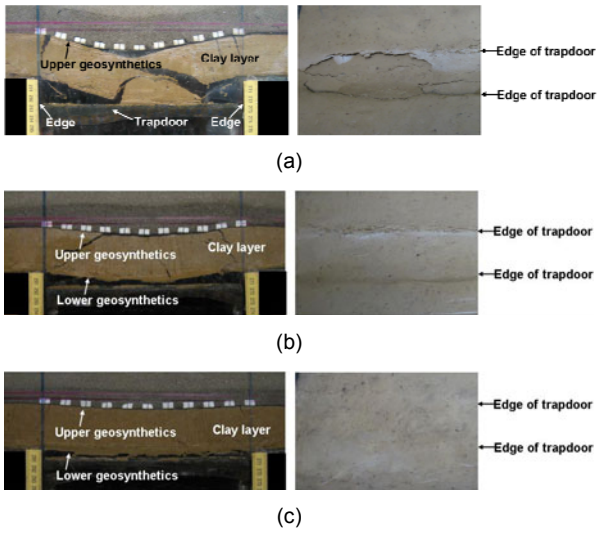

Fig. 17 Deformations of geosynthetics and compacted clay layers

Side view and top view of compacted clay layer for Test 7 (a), Test 8 (b), and Test 9 (c)

Fig. 18 shows the effect of the compacted clay layer on deflection and strain of the upper geosynthetics. The maximum deflections of the upper geosynthetics in Test 8 and Test 9 are 8.95 mm and 5.80 mm, respectively, which are much lower than those of Test 5 and Test 6. Thus, the compacted clay layer combined with the underlying geosynthetic reinforcement can reduce the deflection and the strain of the upper sealing geosynthetics effectively. The mechanism can be drawn as follows. Firstly, the compacted clay layer and the underlying geosynthetics can form a composite bearing structure like a beam. This kind of structure has a bending rigidity, compared with the tensioned membrane structure. Secondly, the compacted clay layer can act as a buffer or a strain-transition zone (Jang and Montero, 1993), which can further reduce the deflection of the upper geosynthetics.

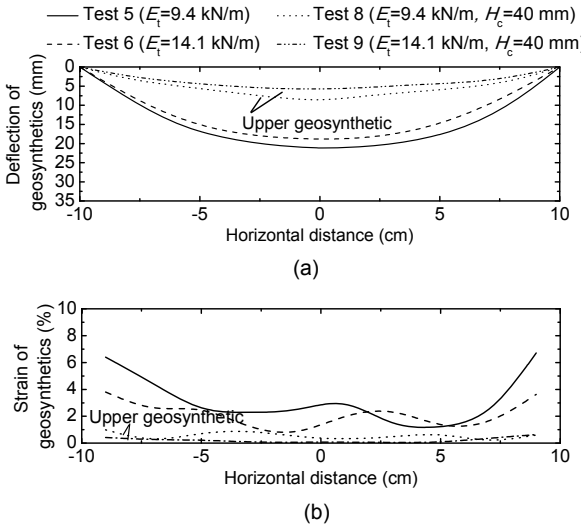

Fig. 18 Effects of compacted clay layer on deflection (a) and strain (b) of upper geosynthetics

4.3 Recommended composite liner structure

For the vertical landfill expansions, reinforcing the composite liner with high strength geosynthetics (i.e., geogrids) is commonly used to accommodate the localized subsidence effects in engineering practices. According to present test results, it is recommended to place a certain thickness of compacted clay layer on the geogrids to further reduce the tensile strains of sealing materials in the composite liner. The recommended structure of the composite liner is shown in

Fig. 19. It includes a geotextile filtration layer, a leachate collection and drainage layer, an impervious layer, a compacted clay layer, and a geosynthetic reinforcement layer.

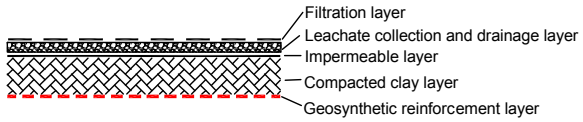

Fig. 19 Recommended composite liner for vertical landfill expansion

5 Conclusions

A series of model tests has been carried out to investigate the soil arching and soil-geosynthetic interaction subjected to localized subsidence in municipal solid waste landfills in the case where the geosynthetic is anchored at the edge of the localized subsidence. The following conclusions can be drawn as follows.

1. The model test results using sandy soil show that soil pressure acting on deflected geosynthetics within the subsidence zone is strongly related to the deflection of the geosynthetics. If the deflection of the geosynthetics is not sufficient to result in a full degree of soil arching, the soil pressure within subsidence zone increases with the increase of filling height. Otherwise, the final soil pressure acting on the deflected geosynthetics would rapidly decrease to reach a minimum value, which appears to be independent of the overburden height.

2. The deflection and strain in the geosynthetics decrease with an increase in its tensile stiffness.

3. In order to reduce the tensile strains of sealing materials, a pragmatic solution is to use a reinforcement layer which combines geosynthetic reinforcements with a compacted clay layer.

4. The present model tests neglect the effect of modulus of filling material and the influence of gravity, which can be studied through centrifugal model tests or full scale tests.

References

ASTM Standard D4595-2009. Standard Test Method for Tensile Properties of Geotextiles by the Wide Width Strip Method. ASTM International, West Conshohocken, PA.

Aubertin, M., Li, L., Arnoldi, S., Simon, R., 2003. Interaction between Backfill and Rock Mass in Narrow Slopes. Soil and Rock Mechanics America, p.1157-1164.

Briançon, L., Villard, P., 2008. Design of geosynthetic-reinforced platforms spanning localized sinkholes. *Geotextiles and Geomembranes*, **26**(5):416-428. [doi:10.1016/j.geotexmem.2007.12.005]

Chen, R.P., Xu, Z.Z., Chen, Y.M., Ling, D.S., Zhu, B., 2010. Field tests on pile-supported embankments over soft ground. *Journal of Geotechnical and Geoenvironmental Engineering*, **136**(6):777-785. [doi:10.1061/(ASCE)GT.1943-5606.0000295]

Chen, R.X., Zhu, B., Chen, Y.M., Chen, R.P., 2010. Modified Terzaghi loosening earth pressure based on theory of main stress axes rotation. *Rock and Soil Mechanics*, **31**(5):1402-1406 (in Chinese).

Chen, Y.M., Cao, W.P., Chen, R.P., 2008. An experimental investigation of soil arching within basal reinforced and unreinforced piled embankments. *Geotextiles and Geomembranes*, **26**(2):164-174. [doi:10.1016/j.geotexmem.2007.05.004]

Chew, S.H., Phoon, H.L., Le Hello, B., 2006. Geosynthetic Reinforced Piled Embankment-Large-Scale Model Tests and Numerical Modeling. 8th International Conference on Geosynthetics, Kuwano, J., Koseki J. (Eds.), Yokohama, Japan, p.901-904.

van Eekelen, S.J.M., Van, M.A., Bezuijen, A., 2007. The Kyoto Road, a Full-Scale Test, Measurements and Calculations. 14th European Conference on Soil Mechanics and Geotechnical Engineering, Madrid, Millpress, Rotterdam, p.1533-1538.

Giroud, J.P., Bonaparte, R., Beech, J.F., Gross, B.A., 1990. Design of soil layer-geosynthetic systems overlying voids. *Geotextiles and Geomembranes*, **9**(1):11-50. [doi:10.1016/0266-1144(90)90004-V]

Handy, R.L., 1985. The arch in soil arching. *Journal of Geotechnical Engineering*, **111**(3):302-318. [doi:10.1061/(ASCE)0733-9410(1985)111:3(302)]

Hu, M.Y., Chen, Y.M., 2001. Engineering aspects of landfilling municipal solid waste. *Journal of Zhejiang University*, **2**(1):34-40. [doi:10.1631/jzus.2001.0034]

Jang, D.J., Montero, C., 1993. Design of liner systems under vertical expansions: an alternative to geogrids. *Proceedings of Geosynthetics*, **3**:1487-1510.

Jessberger, H.L., Stone, K.J.L., 1991. Subsidence effects on clay barriers. *Geotechnique*, **41**(2):185-195. [doi:10.1680/geot.1991.41.2.185]

Kuo, S.S., Desai, K., Rivera, L., 2005. Design method for municipal solid waste landfill liner system subjected to sinkhole cavity under landfill site. *Practice Periodical of Hazardous, Toxic, and Radioactive Waste Management*, **9**(4):281-291. [doi:10.1061/(ASCE)1090-025X(2005)9:4(281)]

Qian, X.D., Koerner, R.M., Gray, D.H., 2001. Geotechnical Aspects of Landfill Design and Construction. Prentice-Hall Inc, New Jersey.

Terzaghi, K., 1943. Theoretical Soil Mechanics. John Wiley and Sons, Inc, New York, p.37-42.

Villard, P., Briançon, L., 2008. Design of geosynthetic reinforcements for platforms subjects to localized sinkholes.

Canadian Geotechnical Journal, **45**(2):l96-209.

Viswanadham, B.V.S., Mahajan, R.R., 2007. Centrifuge model tests on geotextile-reinforced slopes. *Geosynthetics International*, **14**(6):365-378. [doi:10.1680/gein.2007.14.6.365]

Zhan, L.T., Chen, Y.M., Lin, W.A., 2008. Shear strength characterization of municipal solid waste at the Suzhou Landfill, China. *Engineering Geology*, **97**(3-4):97-111. [doi:10.1016/j.enggeo.2007.11.006]

Zhu, B., Chen, R.X., Chen, Y.M., Gao, D., 2009. Action mechanism and design method of horizontal reinforcement subjected to trench void. *China Journal of Highway and Transport*, **22**(1):11-16 (in Chinese).

Zornberg, J.G., Arriaga, F., 2003. Strains distribution within geosynthetic-reinforced slopes. *Journal of Geotechnical and Geoenvironmental Engineering*, **129**(1):32-45. [doi:10.1061/(ASCE)1090-0241(2003)129:1(32)]